THE ASTROPHYSICAL JOURNAL, 452:933–943, 1995 October 20


# GAMMA-RAY MEASUREMENTS OF FLARE-TO-FLARE VARIATIONS IN AMBIENT SOLAR ABUNDANCES

GERALD H. SHARE AND RONALD J. MURPHY
E.O. Hulburt Center for Space Research, Code 7650, Naval Research Laboratory, Washington, DC 20375
*Received 1995 February 14; accepted 1995 May 1*

## ABSTRACT

We have measured fluxes of 10 narrow $\gamma$-ray lines in 19 X-class solar flares observed by the *Solar Maximum Mission* spectrometer from 1980 to 1989. These lines originate from interaction of energetic protons and $\alpha$-particles with ambient solar material. Flare-to-flare variations in line fluxes reveal that the abundances of elements in the flare plasma are grouped with respect to their first ionization potentials (FIPs). Line fluxes from elements with similar FIPs correlate well with one another; in contrast, the low-FIP ($<10$ eV; e.g., Mg, Si, and Fe) to high-FIP ($>11$ eV; e.g., C, N, and O) line ratios vary by as much as about a factor of 4 from flare to flare. This factor of 4 is consistent with the enhancement of low-FIP elements found in the solar corona relative to photospheric abundances. We also find that the Ne/O line ratio increases as the accelerated particle spectrum becomes softer. This can be explained by excitation cross sections less than 10 MeV, but the magnitude of the effect is dependent on the accelerated $\alpha$-particle/proton ratio. After correcting for this spectral dependence, we find that the Ne/(C+N+O) line ratio is constant from flare-to-flare, indicating that Ne behaves like these other high-FIP elements in the ambient flare plasma. We discuss a possible explanation, which is based on these observations, for the factor of $\sim 3$ enhancement in the abundance of Ne relative to other high-FIP elements in the 1981 April 27 flare found by Murphy et al. (1991).

*Subject headings:* Sun: abundances — Sun: flares — Sun: particle emission — Sun: X-rays, gamma rays

## 1. INTRODUCTION

Gamma-ray line observations provide measurements of the elemental abundances of ambient solar material and of the accelerated particle composition and spectra in solar flares. Preliminary analysis (Forrest 1983) of the 1981 April 27 spectrum accumulated by the gamma-ray spectrometer (GRS) on the *Solar Maximum Mission* (*SMM*) suggested that line emissions from the heavy elements, such as Fe, Mg, Si, and Ne, were present in significantly higher proportion relative to emissions from lighter elements, such as C and O, than expected for photospheric abundances. This study was based on lines with relatively "narrow" widths, instrumentally resolved and moderately Doppler-broadened, produced by interaction of protons and $\alpha$-particles on ambient solar material (e.g., de-excitation lines at 1.634 MeV from Ne and at 4.439 MeV from C). These lines are distinguished from "broad" ($\sim 1$ MeV width) features that arise from (1) a multitude of blended and weak narrow lines and (2) highly Doppler-broadened lines produced by interaction of accelerated heavy nuclei (e.g., C and Fe) with ambient hydrogen and helium.

Murphy et al. (1991) performed detailed fits to the April 27 spectrum for assumed accelerated particle spectra and for different compositions of both the accelerated particles and ambient medium. They used nuclear cross sections and kinematical calculations to obtain the best fitting solar flare parameters for a thick-target interaction model. Their analysis suggests that the ambient elemental ratios Mg/C, Si/C, and Fe/C are similar to those typically found in the corona and $\sim 3$ times higher than those in the photosphere.

Observations of solar energetic particles and the solar wind led Meyer (1985a, b) to conclude that elements separate based on the level of their first ionization potential (FIP). Those elements with potentials exceeding $\sim 11$ eV fall into the high-FIP category (e.g., C, N, O, and Ne) and those below $\sim 10$ eV fall into the low-FIP category (e.g., Mg, Si, and Fe). Meyer reviewed earlier spectroscopic measurements of solar plasmas and found agreement with this enhancement of low-FIP elements in the upper solar atmosphere. Feldman (1992) reviewed more recent spectroscopic measurements of abundances in the upper atmosphere that confirmed Meyer's findings. However, he also noted that the relative enhancement of the low-FIP elements can vary from region to region by more than a factor of 10 (Widing & Feldman 1993). Dere et al. (1982) also showed that the Si IV/C IV intensity ratio is 3 times higher above an active region than it is above a nearby sunspot. An electromagnetic field is assumed to transfer the ionized elements into the upper atmosphere (Feldman 1992); however, the strong and predominantly horizontal magnetic fields in the region of the sunspot can trap the ions and prevent them from escaping. Antiochos (1994) suggests that the low-FIP enhancement in the corona can be explained by chromospheric evaporation. Elemental abundances in flare plasmas also appear to be highly variable. Feldman & Widing (1990) used *Skylab* XUV data from an M1 flare in 1973 to infer that the elemental abundances of the flare plasma were consistent with those found in the photosphere; on the other hand, Feldman (1990) reviewed abundances in high-temperature regions of large flares and found them to be consistent with those found in the corona. Meyer (1993) provides a comprehensive summary of all the solar abundance measurements; Reames (1995) summarizes the latest measurements of coronal abundances from studies of energetic solar particles.

The $\gamma$-ray analysis revealed an additional puzzle that the FIP separation model does not explain. Murphy et al. (1991) found an unexpected enhancement of ambient Ne (FIP = 21.6 eV) relative to the other high-FIP elements compared to both

coronal and photospheric abundances. This indicates that either the FIP model is not correct or that some other process concentrates Ne in flare plasma. Shemi (1991) suggested that the Ne is photoionized by intense soft X-rays emitted during extended flares, thus allowing it to preferentially diffuse, along with the low-FIP elements, into the interaction region. Additional evidence that elevated levels of Ne are found in coronal-type material was presented by Schmelz et al. (1993), who found an excess of Ne over O in measurements made of the X-ray plasma during a relatively intense and impulsive flare (M5 X-ray classification); however, she found no such enhancement of Ne in a weaker flare (M1) with more gradual rise and fall. Studies of solar energetic particles have also revealed significantly elevated Ne/O ratios in the impulsive $^3$He-rich flares (Reames, Ramaty, & von Rosenvinge 1988); however, this enhancement is believed to be due to dependence of the acceleration process on the ionization state of the elements in the preflare plasma and not to any enhanced abundance of Ne in the corona (Reames, Meyer, & Von Rosenvinge 1994). In fact, coronal abundances derived from the gradual solar events are in agreement with spectroscopic measurements of the corona.

In this paper we extend an empirical technique developed by Murphy et al. (1990) for the 1981 April 27 flare to study the relative intensities of "narrow" $\gamma$-ray lines in 19 solar flares with intense nuclear emission, observed from 1980 to 1989 by the *SMM* GRS. From these fits we can infer variations in the ambient elemental abundances. A future paper discussing measurements of the composition of the accelerated particles in these flares is in preparation. This technique differs from the rigorous, but more laborious, method which uses nuclear cross sections and relevant kinematics to calculate the incident $\gamma$-ray spectra for comparison with the data (Murphy et al. 1991; see above discussion) and which allows direct determination of the flare-accelerated proton and $\alpha$-particle spectra, ambient elemental abundances, and accelerated particle composition. Application of this latter method to the full flare database is planned.

## 2. METHOD AND ANALYSIS

### 2.1. *Database*

A total of 185 flares were detected above 300 keV by the *SMM* GRS from 1980 to 1989, with sufficient statistics for spectral analysis and with good background subtraction. The spectra were accumulated in 476 logarithmically spaced channels from $\sim$0.3 to 9 MeV (Forrest et al. 1980). A complete catalog of the *SMM* GRS flares is being prepared. The duration of each event was determined by visual inspection of both raw counting rates and background-corrected data. Durations ranged from tens to thousands of seconds. The integrated spectra exclude data with telemetry errors and data obtained during portions of intense flares when the detector was saturated (e.g., the early part of the 1982 June 3 flare). We obtained background-corrected spectra for the flares using two methods. Where possible, we obtained backgrounds 15 orbits before and after the event, where the orbital parameters were close to those during the flare. When only one of the two backgrounds was available, this background correction was occasionally inadequate. This method also failed when flares occurred soon after exposure to protons in the South Atlantic Anomaly because the dosage did not always change in a linear fashion from day to day. For events with durations less than 5 minutes, we could use backgrounds taken just before and after the flare. Only properly corrected spectra have been included in the flare sample.

Spectral channels were summed together to provide adequate statistics for fits using a least-squares analysis. We found that summing the spectra into eight-channel accumulations provided adequate statistics for the fits and did not significantly degrade the ability to accurately measure the intensity in narrow lines, such as the 2.223 MeV line from neutron capture. We also summed data channels in a sequential manner from low to high energies, requiring a minimum 0.5 $\sigma$ significance in the flare counts for a given accumulation; the number of summed channels was not allowed to decrease as we progressed to higher energies. These two spectral summations gave similar results for strong flares.

For purposes of this paper we next screened the flare spectra for evidence of significant nuclear line emission. This was done by simultaneously fitting the time-integrated flare spectra greater than 0.3 MeV with a model consisting of seven components: (1) an electron bremsstrahlung continuum represented by a single, summed, or broken power law, (2) a prompt "narrow" nuclear line component based on a template derived from the 1981 April 27 flare (Murphy et al. 1990; note that the current template differs from that in the cited paper because we have improved the instrument response model), (3) a prompt "broad" nuclear line component based on fits to the same flare, (4) a prompt broad line near 0.450 MeV, which is due to $\alpha$-$\alpha$ interactions, (5) a line at 0.511 MeV, which is due to annihilation radiation, (6) a positronium continuum, and (7) a narrow line at 2.223 MeV which is due to neutron capture on hydrogen.

We are primarily interested in the prompt "narrow" nuclear line component in this paper because this component contains information on the elemental abundance of the flare plasma. Later papers will discuss the results derived from studies of the other components. Of the 185 flares in the database we found 39 that exhibited a "narrow" component with significance greater than 4 $\sigma$ in the integrated spectra. Many of these spectra are too weak for individual line spectroscopy; for this reason we developed a more restricted sample of flares, viz., those with significance greater than 6.5 $\sigma$ in the "narrow"-line component. The 19 flares in this sample are listed in Table 1. We provide the date, the starting time of the spectral integration, the total accumulation time, the location on the Sun, the *GOES* X-ray classification, the optical importance and brightness, and the fluence (time-integrated flux) in the narrow nuclear lines obtained by summing the fluences of the individual de-excitation lines, as described below. We caution the reader that some of the listed nuclear fluences exclude data gaps, occulted portions of the orbit, and periods when the instrument was saturated; for this reason direct comparison with other parameters for these flares is not recommended.

Plotted in Figure 1 are time-integrated spectra for 12 of the 19 flares. The curves drawn through the data points are the best-fit models consisting of the seven components described above. The lines drawn below the data points are best fits to the electron bremsstrahlung continuum. We note that four flares emitted higher fluences of prompt nuclear lines than did the well-studied flare on 1981 April 27. It is also noteworthy that the flare with the most prolific nuclear line emission occurred on 1989 March 6. This is the same flare that exhibited episodes of intense electron-dominated emission (Rieger 1994). As our studies relate to isotropically emitted nuclear $\gamma$-rays

TABLE 1

PARAMETERS OF 19 FLARES USED IN THIS STUDY

| Flare | Date | Start (UT) | Accumulation Time (s) | Location (latitude longitude) | X-Ray Class | Optical | Narrow $\gamma$ Lines ($\gamma$ cm$^{-2}$) |
|---|---|---|---|---|---|---|---|
| 1..... | 1981 Apr 10 | 16:46:13 | 524 | N07 W36 | X 2.3 | 2B | 23.5 ± 3.1[a] |
| 2..... | 1981 Apr 27 | 08:04:01 | 1916 | N16 W90 | X 5.5 | 1N | 113.1 ± 6.2 |
| 3..... | 1982 Jun 3 | 11:42:27 | 1195 | S09 E72 | X 8.0 | 2B | 28.6 ± 6.9[a] |
| 4..... | 1982 Jul 9 | 07:35:24 | 327 | N17 E73 | X 9.8 | 3B | 33.6 ± 3.4 |
| 5..... | 1982 Nov 26 | 02:29:21 | 393 | S11 W87 | X 4.5 | 2B | 16.2 ± 2.7[a] |
| 6..... | 1982 Dec 7 | 23:38:29 | 2703 | S19 W79 | X 2.8 | 1B | 147.9 ± 8.8 |
| 7..... | 1984 Apr 24 | 23:59:26 | 1097 | S11 E45 | X 13.0 | 3B | 55.3 ± 6.2[a] |
| 8..... | 1986 Feb 6 | 06:20:19 | 1228 | S07 W02 | X 1.7 | 2B | 45.4 ± 4.5 |
| 9..... | 1988 Dec 16 | 08:28:50 | 3555 | N27 E33 | X 4.7 | 2B | 219.6 ± 10.7 |
| 10..... | 1989 Mar 6 | 13:56:23 | 3515 | N33 E71 | X 15.0 | 3B | 293.8 ± 11.6 |
| 11..... | 1989 Mar 10 | 19:03:40 | 3341 | N32 E22 | X 4.5 | 3B | 108.5 ± 7.5[a] |
| 12..... | 1989 Mar 17 | 17:31:22 | 835 | N33 W61 | X 6.5 | 2B | 48.8 ± 4.6 |
| 13..... | 1989 May 3 | 03:42:49 | 1376 | N28 E32 | X 2.3 | 3B | 24.3 ± 4.1 |
| 14..... | 1989 Aug 16 | 01:22:56 | 916 | S15 W85 | X 20.0 | 2N | 45.9 ± 3.9[a] |
| 15..... | 1989 Aug 17 | 00:47:52 | 2228 | S17 W88 | X 2.9 | SN | 54.4 ± 7.3 |
| 16..... | 1989 Sep 9 | 09:09:51 | 541 | N17 E30 | X 1.4 | 1B | 17.0 ± 2.9 |
| 17..... | 1989 Oct 19 | 12:56:39 | 3260 | S25 E09 | X 13.0 | 3B | 179.7 ± 10.3[a] |
| 18..... | 1989 Oct 24 | 17:53:18 | 819 | S29 W57 | X 5.7 | 2N | 44.7 ± 3.7[a] |
| 19..... | 1989 Nov 15 | 19:33:15 | 1016 | N16 W27 | X 1.8 | 2B | 32.6 ± 4.4 |

[a] Partial measurement.

from excitation of the ambient medium at modest atmospheric depths, we do not expect a significant dependence on heliocentric angle. Close inspection of the spectra reveals that the line intensities depart significantly from the April 27 nuclear line template (e.g., the 1988 December 16 flare). This difference prompted us to fit the individual nuclear lines separately. This is described in the next section.

### 2.2. *Narrow-Line Fits*

The "narrow" nuclear component is comprised of 10 line features identified by Murphy et al. (1990). Table 2 lists eight of these features and estimates of the fractional contributions to each feature from specific solar elements based on abundances derived from the 1981 April 27 flare (Ramaty, Kozlovsky, & Lingenfelter 1979; Ramaty & Kozlovsky 1994). Note that although the listed energies of the features are those of the primary de-excitation line, other lines not resolvable by the spectrometer and at slightly different energies may also contribute to the measured line strength. Spallation of heavier elements contribute to the lines for harder accelerated particle spectra. The percentages listed are for Bessel function proton and $\alpha$-particle spectra with $\alpha T$ parameters ranging from 0.01 to 0.05, estimated from fits to the data (Ramaty et al. 1993). The moderately broadened line at 1.02 MeV and the broad complex of lines near 5.3 MeV identified by Murphy et al. (1990) are not included in the table. The source of the 1.02 MeV feature has not been identified; lines from N and O contribute to the ~5.3 MeV feature. The lines in the table, with the exception of those at 1.238 and 4.439 MeV lines, are dominated by de-excitation from a single element; for this reason we are able to deduce flare-to-flare abundance variations from the line measurements.

TABLE 2

ELEMENTAL CONTRIBUTIONS TO GAMMA-RAY LINES IN PERCENT

| | Line Energy (MeV) | | | | | | | |
|---|---|---|---|---|---|---|---|---|
| Element | 0.847 | 1.238 | 1.369 | 1.634 | 1.778 | 4.439 | 6.129 | ~7 |
| C..... | ... | ... | ... | ... | ... | 65–35 | 0–1 | 1–3 |
| N..... | ... | ... | ... | 4–3 | ... | 3–12 | ... | ... |
| O..... | ... | ... | ... | 0–4 | ... | 32–53 | 97–90 | 92–93 |
| Ne ..... | ... | 30–12 | ... | 91–69 | ... | ... | 3–9 | ... |
| Mg..... | 2–6 | ... | 91–78 | 4–18 | 5–4 | ... | ... | ... |
| Si..... | 1–8 | 37–10 | 2–19 | 1–6 | 86–82 | ... | ... | 7–4 |
| S ..... | ... | 0–3 | ... | ... | 0–1 | ... | ... | ... |
| Fe..... | 97–86 | 33–75 | 7–3 | ... | 9–13 | ... | ... | ... |

We used the same fitting procedure described in Murphy et al. (1990), called the "hypothesis testing" method. In this approach a trial incident spectrum is constructed and convolved with a numerical model of the instrumental response. The resulting predicted counts are compared, channel by channel, with the observed spectral data. We have used a recently improved instrument response function that does a better job reproducing the pair escape peaks and Compton continuum observed in calibrations of the spectrometer and flare spectra. A $\chi^2$ minimization algorithm was used to fit the data. In order to constrain the fits, we have fixed the line center energies and widths of the 10 prompt "narrow" lines, the five prompt "broad" lines, the $\alpha$-$\alpha$ line, the positron annihilation line, and the neutron capture line at their theoretical values listed in Murphy et al. (1990). Free parameters in the fits are the amplitudes of the 18 lines, and the amplitudes and exponents of single, summed, or broken power laws used to describe the bremsstrahlung continuum. In order to simplify the fit we did not include the positronium continuum in the model; this does not affect the amplitudes of the higher energy lines. Fits for 12 of the 19 flares provided acceptable values of $\chi^2$ per dof (greater than 5% probability). The seven flares with unacceptable fits (maximum $\chi^2$ per dof was 1.7) were the most intense. It is clear that our relatively simple model is inadequate to describe these high-statistics data, especially below 1 MeV. The relatively poor fits at these lower energies do not significantly impact the line measurements, which are of interest to us in this paper.

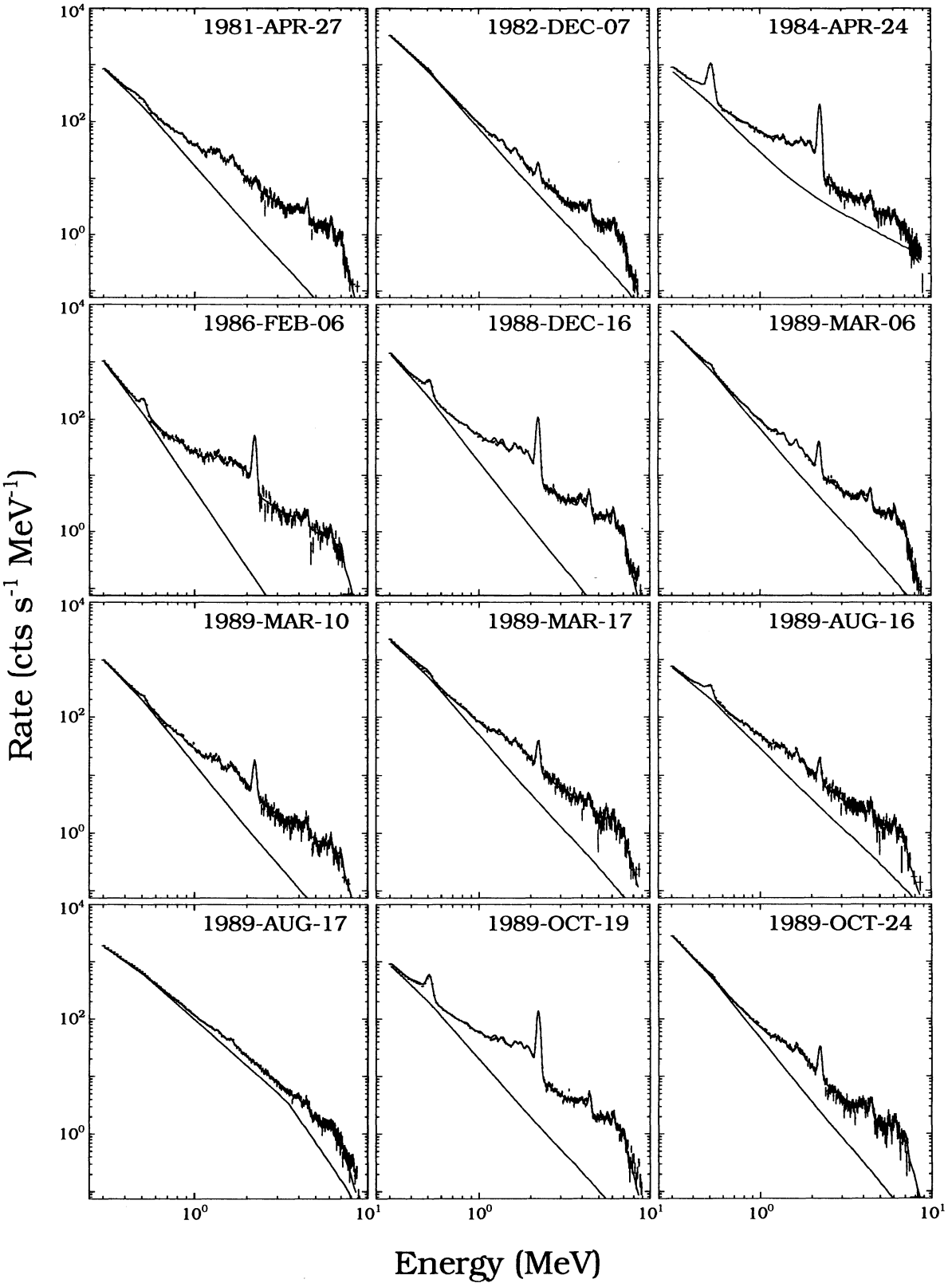


FIG. 1.—Spectra of 12 of the $\gamma$-ray line flares studied. Solid curves drawn through the data points are the best-fit models; the fitted bremsstrahlung component is shown by the curves beneath the data points.

## 3. RESULTS

Listed in Table 3 are the results of our fits for the 19 flares. Relative intensities are provided for all 10 lines as a percentage of the total prompt narrow-line fluence (i.e., the sum of the 10 lines) given in Table 1. We note that the relative line strengths for the 1981 April 27 flare differ from those reported by Murphy et al. (1990) because we have used a modified instrument response (see § 2.2). Only the value for the 4.43 MeV/6.13 MeV line ratio differs significantly ($\sim 2.5\ \sigma$) from the earlier value. This does not affect the flare-to-flare results we report in this paper; however, it does provide an indication of the systematic uncertainty in determining the relative elemental abundances using the *SMM* $\gamma$-ray data. We focus our discussion on the eight strongest lines found in the flare spectra and ignore the features near 1.02 and 5.3 MeV. We note that the feature near 1.02 MeV comprised, on average, only 3% of the narrow nuclear fluence and was only marginally detectable, if at all, in most flares. The broad and complex feature near 5.3 MeV also only accounted for typically less than 5% of the prompt narrow nuclear fluence in the flares.

### 3.1. *FIP Abundance Variations*

Since elemental abundances in various solar regions have been shown to be dependent on first ionization potential (FIP), it makes sense to study the flare-to-flare line variability using this grouping. From Table 2 we see that the lines at 0.85, 1.24, 1.37, and 1.78 MeV are dominated by emissions from low-FIP (< 10 eV) elements Mg, Si, and Fe. (Note that the high-FIP element $^{22}$Ne, ~9.2% natural abundance, has a direct excitation line at 1.275 MeV, which is one instrumental half-width at half-maximum from 1.24 MeV and could contribute to the measured intensity of the Fe line.) The lines near 4.43, 6.13, and ~7 MeV are dominated by emissions from high-FIP elements C, N, and O. The line at 1.634 MeV is dominated by emission from high-FIP element Ne, but can contain a contribution from low-FIP Mg.

We seek to establish whether the 19 flare sample of *SMM* $\gamma$-ray observations supports this grouping by FIP in the flare plasma. We study the relative fluxes of lines emitted by elements with (1) low FIP (< 10 eV) and (2) high FIP (> 11 eV), excluding the 1.634 MeV line from Ne. We then compare the summed fluxes of low- and high-FIP lines to determine whether their ratio varies from flare to flare. Last, we study how well the 1.634 MeV (Ne) line correlates with those of the high- and low-FIP lines; this will determine whether Ne has the same behavior as other high-FIP elements in the flare plasma.

In order to study the low-FIP elements, we have summed the fluxes of lines at 0.847, 1.238, and 1.778 MeV associated with emission from Fe (FIP = 7.9 eV) and Si (8.2 eV). In Figure 2*a* we compare these summed fluxes with those from the 1.369 MeV line associated with Mg (7.6 eV); they are strongly correlated (correlation coefficient $r = 0.87$). Similar, but less statistically significant results, were obtained when the three lines were individually compared with the 1.369 MeV line. The line drawn through the points in Figure 2*a* is the slope determined by fitting the (0.85 + 1.24 + 1.78) MeV/1.369 MeV line ratios, plotted in Figure 2*b*, to a constant. The flare-to-flare variation of this ratio is small, relative to the statistical uncertainties. We can quantify how well these line fluxes are correlated by using the $\chi^2$ statistic applied to the ratios; however, because the uncertainties in the ratios are proportional to their values, this test can give spurious results. For this reason we also calculated the quantity $(A-B)/(A+B)$, where $A$ and $B$ are the line fluxes for each flare, and again tested for constancy from flare-to-flare. We find that between 80% and 90% of randomly distributed samples about a mean have values of $\chi^2$ greater than what was observed in these two tests. Within the limited statistics of our $\gamma$-ray line measurements, we conclude that the relative abundances of low-FIP elements Mg, Si, and Fe are correlated in flares.

We next study how well line intensities associated with high-FIP elements, C (FIP = 11.3 eV), N (14.5 eV), and O (13.6 eV) correlate with one another. We treat separately the 1.634 MeV line, arising primarily from de-excitation of high-FIP Ne (21.6 eV), because of the anomalous Ne abundance found in earlier analyses of the 1981 April 27 flare (e.g., Murphy et al. 1991). Plotted in Figure 2*c* is a comparison of the fluxes of the 4.43

TABLE 3

RELATIVE LINE FLUXES FOR 19 FLARES

| | LINE ENERGY (MeV) | | | | | | | | | |
|---|---|---|---|---|---|---|---|---|---|---|
| FLARE | 0.847 | ~1.02 | 1.238 | 1.369 | 1.634 | 1.778 | 4.439 | ~5.3 | 6.129 | ~7 |
| 1..... | 8.7 ± 4.7 | −1.1 ± 3.6 | 7.7 ± 4.0 | 18.0 ± 5.4 | 27.6 ± 4.6 | 9.8 ± 4.4 | 9.5 ± 3.4 | 1.7 ± 2.5 | 13.4 ± 2.1 | 4.6 ± 2.0 |
| 2..... | 4.2 ± 2.0 | 4.5 ± 1.6 | 9.6 ± 1.8 | 12.9 ± 2.4 | 17.3 ± 2.1 | 6.3 ± 2.0 | 16.7 ± 1.7 | 5.5 ± 1.2 | 12.9 ± 1.0 | 10.3 ± 0.9 |
| 3..... | 6.5 ± 8.0 | −8.1 ± 6.8 | 3.9 ± 7.5 | 15.9 ± 9.0 | 28.3 ± 8.4 | 7.7 ± 7.9 | 33.2 ± 5.2 | −1.3 ± 3.6 | 7.8 ± 2.8 | 6.1 ± 2.8 |
| 4..... | 9.8 ± 3.9 | −3.8 ± 2.9 | 7.2 ± 3.1 | 15.9 ± 3.9 | 16.9 ± 3.5 | 17.2 ± 3.4 | 15.3 ± 2.9 | 0.9 ± 2.0 | 13.4 ± 1.7 | 7.1 ± 1.6 |
| 5..... | 16.7 ± 6.4 | 4.2 ± 4.9 | 8.6 ± 5.4 | 13.3 ± 6.9 | 12.0 ± 6.1 | 6.4 ± 5.8 | 6.6 ± 4.5 | 6.3 ± 3.3 | 11.5 ± 2.7 | 14.5 ± 2.8 |
| 6..... | −0.9 ± 2.1 | 0.3 ± 1.6 | 8.0 ± 1.7 | 14.8 ± 2.1 | 23.9 ± 1.9 | 8.6 ± 1.7 | 18.0 ± 1.5 | 3.9 ± 1.1 | 14.7 ± 0.9 | 8.7 ± 0.8 |
| 7..... | 7.3 ± 3.4 | −4.6 ± 2.7 | 1.7 ± 3.1 | 17.2 ± 3.9 | 25.4 ± 3.6 | 13.1 ± 3.6 | 21.6 ± 2.8 | 0.3 ± 2.1 | 12.1 ± 1.8 | 5.8 ± 1.7 |
| 8..... | 6.1 ± 3.7 | 6.6 ± 2.9 | 3.1 ± 3.3 | 20.5 ± 4.2 | 14.4 ± 3.7 | 3.6 ± 3.7 | 14.3 ± 2.6 | 7.4 ± 1.9 | 16.6 ± 1.6 | 7.4 ± 1.5 |
| 9..... | 3.4 ± 1.4 | 1.0 ± 1.1 | 2.7 ± 1.3 | 8.1 ± 1.5 | 23.6 ± 1.5 | 4.8 ± 1.5 | 21.2 ± 1.2 | 5.0 ± 0.9 | 19.8 ± 0.8 | 10.4 ± 0.7 |
| 10..... | 6.4 ± 1.3 | −0.2 ± 0.9 | 4.3 ± 1.0 | 15.2 ± 1.2 | 21.8 ± 1.1 | 9.3 ± 1.1 | 16.6 ± 1.0 | 4.0 ± 0.7 | 13.6 ± 0.6 | 9.0 ± 0.6 |
| 11..... | 6.0 ± 2.6 | 6.2 ± 1.9 | 8.4 ± 2.3 | 15.1 ± 2.6 | 20.8 ± 2.5 | 8.4 ± 2.4 | 12.9 ± 2.0 | 3.0 ± 1.4 | 11.8 ± 1.2 | 7.3 ± 1.2 |
| 12..... | −0.4 ± 3.4 | 6.4 ± 2.6 | 11.2 ± 2.9 | 16.2 ± 3.3 | 19.3 ± 3.2 | 6.6 ± 3.1 | 13.5 ± 2.7 | 3.5 ± 1.9 | 14.6 ± 1.6 | 9.1 ± 1.5 |
| 13..... | 6.6 ± 6.4 | 7.7 ± 5.0 | −2.2 ± 5.9 | 16.8 ± 7.1 | 23.7 ± 6.5 | 2.0 ± 6.3 | 13.6 ± 5.1 | 4.6 ± 3.4 | 17.3 ± 2.9 | 10.0 ± 2.8 |
| 14..... | 6.3 ± 3.0 | 3.2 ± 2.4 | 4.2 ± 2.7 | 13.2 ± 3.0 | 25.0 ± 3.0 | 10.3 ± 2.8 | 13.4 ± 2.7 | 1.9 ± 2.0 | 13.9 ± 1.7 | 8.5 ± 1.7 |
| 15..... | 3.7 ± 5.3 | 4.3 ± 4.2 | 4.4 ± 4.5 | 13.6 ± 4.9 | 33.0 ± 4.8 | −0.4 ± 4.5 | 21.2 ± 4.2 | −0.9 ± 2.8 | 15.0 ± 2.5 | 6.1 ± 2.4 |
| 16..... | 5.2 ± 6.4 | −6.5 ± 4.9 | 9.0 ± 5.9 | 26.7 ± 6.9 | 11.3 ± 6.4 | 11.6 ± 6.3 | 11.5 ± 5.2 | 0.5 ± 3.8 | 22.6 ± 3.4 | 8.1 ± 3.0 |
| 17..... | 2.7 ± 1.5 | 2.4 ± 1.2 | 1.3 ± 1.4 | 10.7 ± 1.6 | 23.2 ± 1.6 | 8.3 ± 1.6 | 20.1 ± 1.4 | 5.2 ± 1.0 | 17.6 ± 0.9 | 8.5 ± 0.8 |
| 18..... | −4.0 ± 3.2 | 6.4 ± 2.5 | 7.7 ± 2.7 | 7.4 ± 3.0 | 22.5 ± 3.1 | 10.3 ± 2.9 | 17.8 ± 2.6 | 4.0 ± 1.8 | 18.9 ± 1.6 | 9.2 ± 1.5 |
| 19..... | 1.9 ± 4.7 | 3.1 ± 3.6 | 12.9 ± 4.4 | 10.0 ± 4.9 | 17.5 ± 4.6 | 1.9 ± 4.5 | 20.0 ± 4.2 | 10.3 ± 3.1 | 12.8 ± 2.5 | 9.6 ± 2.6 |

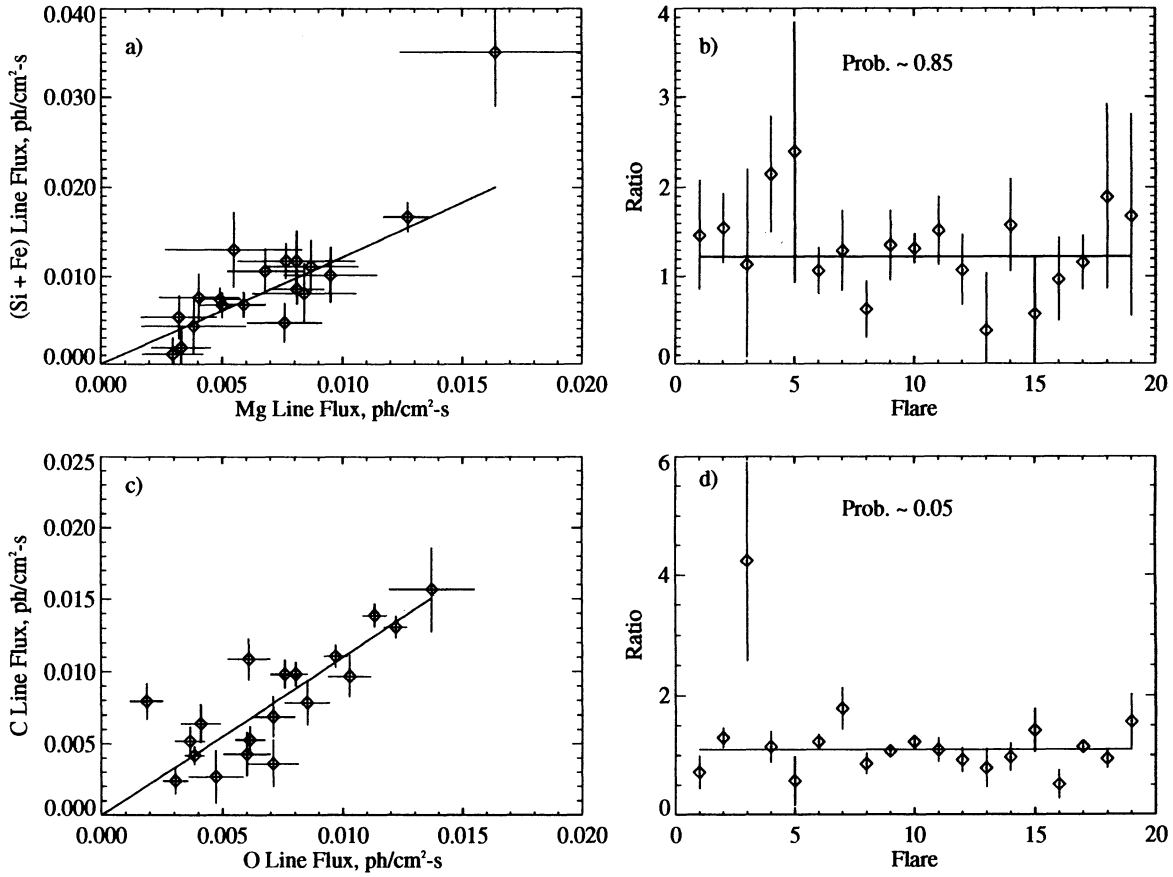


FIG. 2.—Comparison of $\gamma$-ray line fluxes from 19 flares illustrating grouping by first ionization potential (FIP). (*a*) Sum of 0.847, 1.238, 1.778 MeV lines from low-FIP Fe and Si vs. the 1.37 MeV line from low-FIP Mg. (*b*) (Fe+Si)/Mg line ratios; ratios are randomly distributed about the weighted mean, shown by the line. (*c*) The 4.43 MeV line from high-FIP C vs. the 6.13 MeV line from high-FIP O. (*d*) C/O line ratios; ratios are randomly distributed about the weighted mean if the June 3 flare (flare 3) is excluded (see text).

MeV C line with those of the 6.13 MeV O line. The fluxes are well correlated ($r = 0.80$), indicating that the abundances of high-FIP elements C and O are correlated in flares. While the fluxes are correlated, there is a relatively large spread in the distribution of ratios around the best-fit slope plotted in Figure 2*d*. Only about 5% of randomly distributed samples about a mean will have values of $\chi^2$ greater than observed with these data. Part of this spread could be due to variations in the spectra of accelerated particles. For example, a harder spectrum can produce a significant increase in the 4.43 MeV line due to spallation products of O. The large ratio of the third data point is for the 1982 June 3 flare, which had a sufficiently hard proton spectrum to produce $\pi^0$ $\gamma$-rays. If we exclude this flare from the sample, the probability that the data are derived from a random distribution about a mean rises to $\sim$20%.

We can test whether the C/O line ratio for other flares is correlated with hardness of the accelerated particle spectrum. Estimates of spectral indices for an assumed power law have been obtained for nine of the 19 flares at heliocentric angles less than 80°, for which complete data are available. These estimates are based on our measurements of the 2.223 MeV neutron capture line and 4.43 MeV carbon de-excitation line. Fluences of the 2.223 MeV line for the nine flares are given in Table 4. Fluences of the 4.43 MeV line can be derived by multiplying the percentages given in Table 3 with the total narrow nuclear line fluences for these flares given in Table 1.

We used calculations of 2.223 MeV/4.43 MeV line ratios for ambient matter and accelerated particles with photospheric abundances, and for isotropic particle distributions given in Murphy (1985; also provided by Ramaty 1994). The derived spectral indices are dependent on the composition of the accelerated particles and the ambient material, as well as on the angular distributions of these particles (Ramaty et al. 1993). Since we are only interested in determining whether the flare-to-flare C/O line ratio has a spectral dependence, our choice of model is not critical.

TABLE 4

2.223 MeV NEUTRON CAPTURE LINE FLUENCES FOR NINE FLARES

| Date | Fluence ($\gamma$ cm$^{-2}$) |
|---|---|
| 1982 Jul 9 | 22.0 ± 1.2 |
| 1982 Dec 7 | 41.6 ± 2.8 |
| 1986 Feb 6 | 95.7 ± 2.0 |
| 1988 Dec 16 | 616.6 ± 5.4 |
| 1989 Mar 6 | 179.9 ± 4.2 |
| 1989 Mar 17 | 36.0 ± 1.7 |
| 1989 May 3 | 21.8 ± 1.5 |
| 1989 Sep 9 | 42.3 ± 1.3 |
| 1989 Nov 15 | 38.7 ± 1.6 |

Shown in Figure 3*a* are the 4.43 MeV/6.13 MeV line ratios plotted versus spectral index. We would have expected to observe an increase in the C/O line ratio with increase in spectral hardness had production of C from O which was due to spallation been important for these flares, as it apparently was for the 1982 June 3 flare. No such increase is observed. In fact, the C/O line ratio appears to decrease with increasing spectral hardness (correlation coefficient $-0.71$). The line is the best-fit slope, assuming a linear relationship between the ratio and index; the slope is significant at $\sim 2.3\ \sigma$. Such a spectral dependence may be explained by investigating the cross sections for direct excitation. Cross sections for exciting Ne, O, and C by interactions with energetic protons and $\alpha$-particles (Ramaty, Kozlovsky, & Lingenfelter 1979) are plotted in Figure 4. We note that the carbon line is excited at significantly lower energies than is the oxygen line for excitation by protons. Such a clear difference in the cross sections, which could give rise to the observed C/O spectral dependence, is not evident under excitation by $\alpha$-particles. Thus, a power-law spectrum of accelerated particles, with a large proton/$\alpha$-particle ratio less than 10 MeV, could explain a spectral dependence in the C/O ratio (also see discussion in § 4.3). This suggests that the residual spread in the distribution of C/O, plotted in Figure 2*d*, may just be due to spectral variations of the accelerated particles.

The good correlations found for elements within the two FIP groupings contrast sharply with the striking variations found when we compare the summed fluxes in low-FIP lines from Fe, Mg, and Si (0.85, 1.24, 1.37, and 1.78 MeV) with those of the high-FIP lines from C, O, and N (4.43, 6.13, and $\sim 7$ MeV). This is illustrated in Figures 5*a* and 5*b*. The formal correlation between the low- and high-FIP lines is good ($r = 0.68$), but the ratios vary significantly from flare to flare: the probability that the ratios are distributed randomly about a mean value is infinitesimal, less than $10^{-10}$. We can test whether the large spread in low-FIP/high-FIP line ratios is due to a dependence on the spectral hardness of the accelerated protons. Shown in Figure 3*b* is a plot of the low-FIP/high-FIP line ratios versus spectral index for nine flares. There is no evident correlation of the low-FIP/high-FIP ratio and the spectral index of the accelerated particles (correlation coefficient $\sim 0.1$). From this we conclude that the large dispersion in the measured ratios reflects striking changes in the relative abundances of low- and high-FIP elements in the plasma from flare to flare.

### 3.2. *Behavior of the* 1.634 MeV *Line from* Ne

We next study how well the intensities of the 1.634 MeV line, which are due in large part to $\gamma$-rays from excited Ne, correlate with those from the low- and high-FIP groupings discussed above. Comparisons of the Ne line with other high-FIP lines are shown in Figures 5*c* and 5*d*; comparisons with low-FIP lines are shown in Figures 5*e* and 5*f*. It is clear that the fluxes in the Ne line are much better correlated with the high-FIP elements ($r = 0.86$) than with the low-FIP elements ($r = 0.63$). There is also a much larger dispersion in the 1.63 MeV/low-FIP flux ratios; formally there is less than a 0.1% chance that these ratios were derived from the distribution of random values about a mean. On the other hand, there is about a 5% probability that the 1.63 MeV/high-FIP line ratios are derived from a randomly distributed sample about a mean. We note that this probability rises to close to 20% when the first flare is removed from the sample.

This level of confidence is about the same we found in Figure

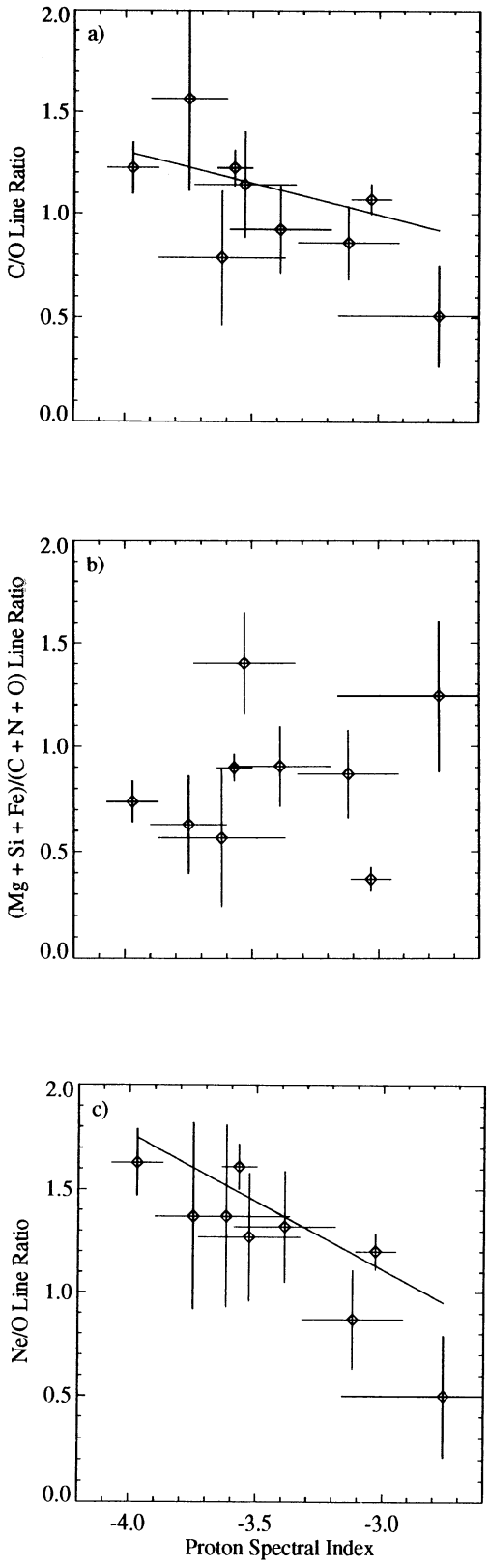


FIG. 3.—Dependence of line ratios on spectral index of accelerated particles for a sample of nine flares. (*a*) C/O line ratio; (*b*) low-FIP (Mg + Si + Fe)/high-FIP (C + N + O) line ratio; (*c*) Ne/O line ratio. Linear weighted least-squares fits are shown by lines. The Ne/O and C/O line ratios reveal a dependence on particle spectrum.

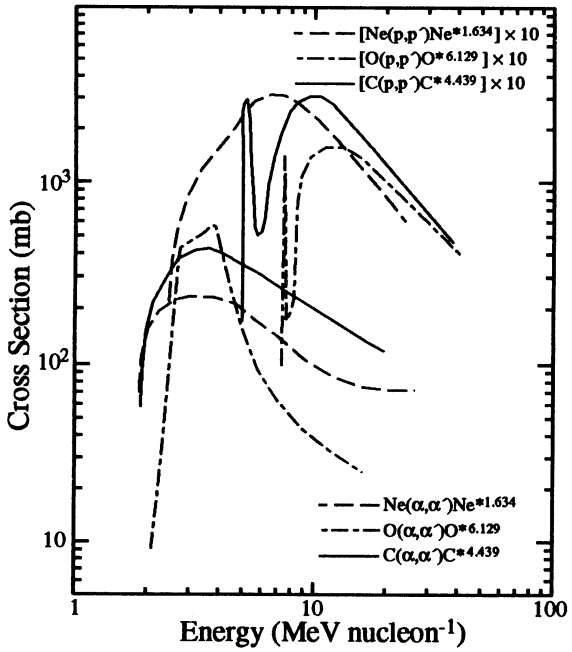


FIG. 4.—Comparison of direct excitation cross sections for Ne, O, and C from interactions with protons (*upper curves*) and α-particles (*lower curves*).

2*d* for variations in the C/O ratio from flare-to-flare. Once again, there is a possible explanation for the spread in Ne/high-FIP line ratios. Referring to Figure 4, we note that Ne can be excited by energetic protons at significantly lower energies than either C or O. Such a clear difference in the cross sections that could give rise to a Ne/O spectral dependence is not evident under excitation by α-particles. Assuming that the $\alpha/p$ ratio is small (e.g., $<0.1$, as shown in Fig. 4), variations in the spectra of accelerated particles could explain the spread in Ne/high-FIP line ratios. This appears to be the case. Plotted in Figure 3*c* is the 1.634 MeV/6.13 MeV line ratio as a function of spectral index. The correlation between this ratio and spectral index is strong (correlation coefficient $-0.88$). The Ne line appears to increase in relative intensity as the spectrum softens. The solid line is the best-fit slope, assuming a linear relationship between the ratio and index; the slope is significant at the $\sim 4\ \sigma$ level. (This occurs in spite of the fact that contributions to the 1.634 MeV line also come from spallation products for harder spectra; see Table 2.) A similar analysis reveals that the Ne/(C+N+O) ratio is also inversely correlated with spectral index at the $\sim 2.5\ \sigma$ level. This reduction in significance is understandable in that the C/O ratio is also apparently spectral dependent. Thus, the spread in the Ne/high-FIP line ratios plotted in Figure 5*d* would have been significantly smaller had we been able to correct for the spectra of the accelerated protons. We therefore conclude that the Ne concentration in flare plasma closely follows those of the other high-FIP elements, C, N, and O.

## 4. DISCUSSION

### 4.1. *Gamma-Ray Lines As Tracers of FIP Enhancements in Flare Plasmas*

We have studied the relative intensities of eight resolved and moderately broadened nuclear γ-ray lines in 19 solar flares. We find that intensities of lines at 0.847 (predominantly from Fe), 1.238 (Fe), 1.369 (Mg), and 1.778 MeV (Si) are well correlated with one another from flare to flare. These four lines originate from elements with first ionization potentials (FIP) less than 10 eV. This suggests that the relative abundances of these low-FIP elements in the ambient flare plasma do not change significantly from flare to flare. However, because of the limited statistical significance of these measurements, we cannot rule out flare-to-flare variations in low-FIP abundances by up to a factor of $\sim 3$ (see Fig. 2*b*). Variations of Mg:Fe abundances by this factor have been inferred from soft X-ray observations of active regions (Saba & Strong 1993). In contrast, McKenzie & Feldman (1992) found Mg:Fe abundance variations of at most 50% in active regions and flare plasmas. Ratios derived in this soft X-ray band are dependent on line emissivity calculations, however (Saba 1995).

We also find a good correlation between intensities of lines at 4.43 MeV (predominantly from C) and 6.13 MeV (O). These two lines originate from de-excitations of elements with FIP $>11$ eV. Some variability is expected in the C/O line ratio because it is dependent on the spectra of the accelerated protons. The C line can be produced by spallation of O by high-energy particles; the high C/O ratio found for the 1982 June 3 flare (Fig. 2*d*) may be due to contributions from spallation. We also show evidence in Figure 3*a* that the C/O line ratio increases as the spectrum of accelerated particles steepens. This increase is consistent with excitation cross sections for proton interactions less than 10 MeV (see discussion in § 4.3 below). We conclude that the data are consistent with a constant abundance ratio of C/O. However, we cannot rule out variations by up to a factor of $\sim 2.5$ which are due to limited statistics (see Fig. 2*d*).

In contrast, we find that the low-FIP/high-FIP (specifically [Mg+Si+Fe]/[C+N+O]) line ratios are highly variable relative to the statistical uncertainties of the measurements (Figs. 5*a*, 5*b*). The relative fluxes of low- and high-FIP lines vary by up to a factor of $\sim 4$ from flare-to-flare. This variation is similar to that observed in ratios of soft X-rays of Fe/Ne and Fe/O in flares (McKenzie & Feldman 1992), Mg/O and Mg/Fe in active regions (Saba & Strong 1993), and with the factor of 4 average enrichment of low-FIP elements in the quiet-Sun upper atmosphere relative to the photosphere (e.g., Meyer 1985).

Our analysis highlights the strong variability in composition of the flare plasma from one flare to another based on FIP of the elements. A more detailed analysis, following the work of Murphy et al. (1991), is required to derive elemental abundances from the γ-ray data directly for all the flares. As discussed in the Introduction, this latter analysis folds in particle spectra, $\alpha/p$ ratios, nuclear cross sections, and kinematics. Plans for this new work are currently being made (Ramaty 1994). The Murphy et al. (1991) analysis of the 1981 April 27 flare revealed a factor of 3 overabundance of low-FIP elements. The ratio of low-FIP/high-FIP line intensities for this flare (second flare in Fig. 5*b*) is close to the average for all flares in the current study. In contrast, the flare on 1988 December 16 (flare 9 in Fig. 5*b*) had a low-FIP/high-FIP ratio at least a factor of 2 lower; this is suggestive of plasma abundances closer to those found in the photosphere.

There are several explanations for this observed variation in the relative concentrations of low-FIP and high-FIP elements in the flare plasma (e.g., Feldman 1992; Meyer 1993): (1) The flare-accelerated ions interact at varying atmospheric depths, from the low chromosphere to low corona, and therefore sample the abundances in these regions directly. (2) Heating in

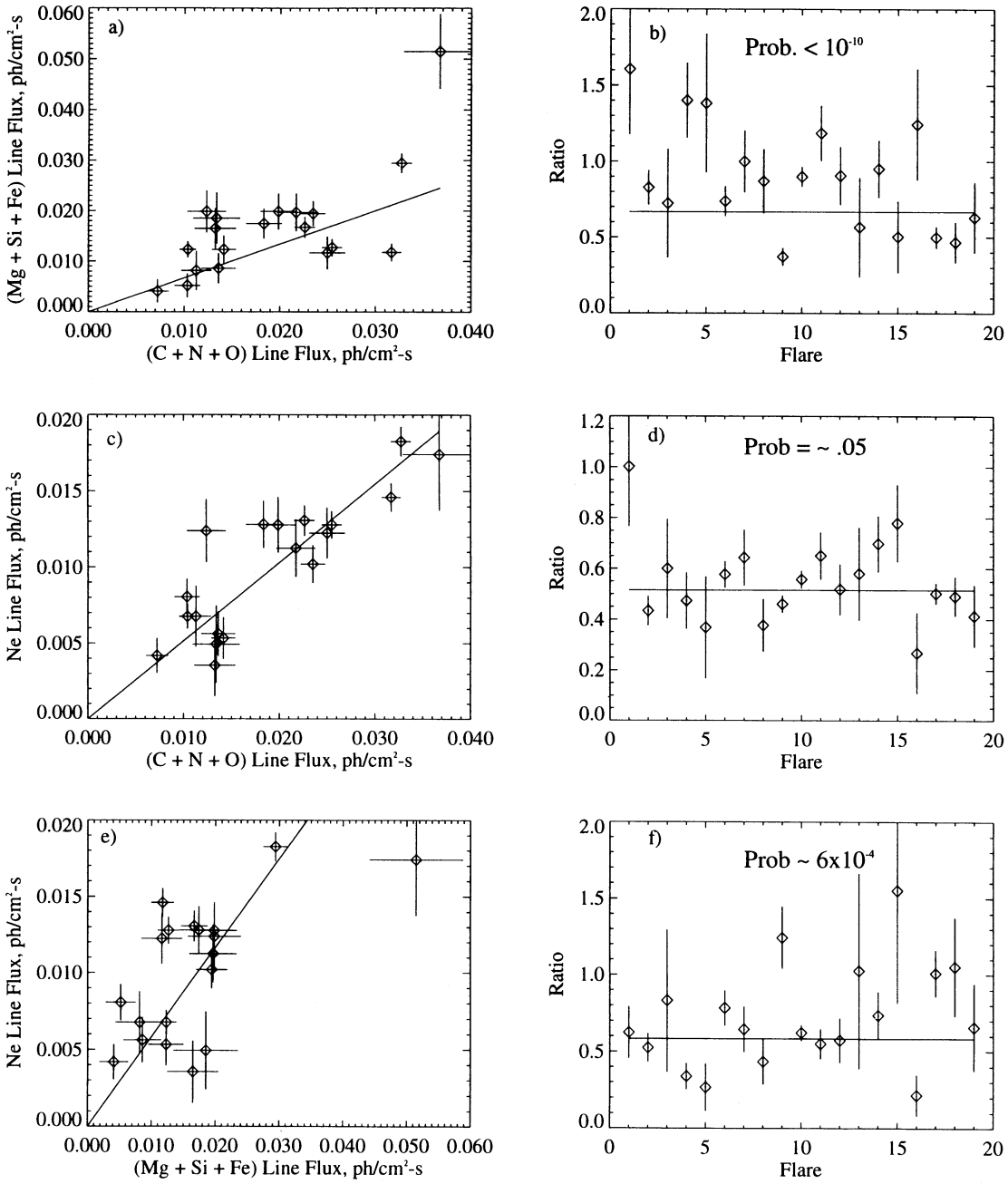


FIG. 5.—(*a*) Comparison of low-FIP (Mg + Si + Fe) line fluxes with high-FIP (C + N + O) fluxes. (*b*) Low-FIP/high-FIP line ratios. (*c*) Comparison of 1.63 MeV (Ne) and high-FIP (C + N + O) line fluxes. (*d*) Ne/high-FIP line ratios. (*e*) Comparison of 1.63 MeV (Ne) and low-FIP (Mg + Si + Fe) line fluxes. (*f*) Ne/low-FIP line ratios. Solid curves are best-fit lines.

the lower chromosphere of active regions could be highly variable such that, in some instances, it is so extreme that all elements are ionized and transported into the flare region; in this case the abundance would appear to be photospheric. In other instances, only the elements with the lowest FIPs are ionized, thus resulting in what appears to be coronal abundances. (3) Because it is known that elemental abundances vary over different regions of the Sun, as a result of magnetic field configurations, the variability may just be due to local conditions that affect the transport of low-FIP elements from the photosphere to the solar atmosphere. Finding temporal variations in the low-FIP/high-FIP ratio during the flares may help to determine the source of the flare-to-flare variability. We plan to search for evidence of this short-term variability in the 19 flares.

### 4.2. Ne *As a High-FIP Element*

Our study of the intensity variations in the 1.634 MeV $\gamma$-ray line demonstrates that Ne behaves like high-FIP elements C, N, and O (Figs. 5*c*, 5*d*) and not like the low-FIP elements (see Figs. 5*e*, 5*f*). The line ratios of Ne/(C + N + O) are consistent with being constant but could still vary by up to a factor of 2. We have shown that much of this variability may be attributed to the dependence of this ratio on the spectrum of the acceler-

ated particles. Recent analysis of EUV data by Widing & Feldman (1995) from nine flares and active regions, and from an erupting prominence, suggests that the O/Ne abundance ratio is relatively constant from photospheric to coronal-type plasmas, as measured by Mg/Ne line ratios. However, they point out that a real change in the O/Ne abundance by a factor of 1.5 is still allowed.

Variations in the inferred O/Ne abundance ratios by factors up to about 2.5 to 3 have been observed in soft X-rays (McKenzie & Feldman 1992; Saba & Strong 1993). Furthermore, Meyer (1993) found a positive correlation in O/Ne and Fe/Ne ratios derived from these soft X-ray observations, suggesting that oxygen behaves like an intermediate-FIP element in active and flaring loops. We have performed a similar analysis using our limited sample of $\gamma$-ray line flares. We have corrected the Ne/(C + N + O) line ratios, plotted in Figure 5*d*, for their apparent dependence on proton spectral index, and plotted them against the low-FIP/high-FIP ratios for the same flares. The results are shown in Figure 6. Based on Meyer's soft X-ray study, one would expect the Ne/(C + N + O) line ratio to fall by about a factor of 2 from photospheric to coronal abundances, as measured by the low-FIP/high-FIP ratio. Limited statistics prevents us from studying this effect with individual flares, but a weighted linear fit to the data indicates that the Ne/(C + N + O) line ratio exhibits only a weak decreasing trend of $(6 \pm 15)\%$ in going from photospheric to coronal abundances. Thus, the $\gamma$-ray line measurements are in better agreement with the EUV observations, which do not reveal a significant change in O/Ne abundance in flares and active regions.

Murphy et al. (1991) have concluded that ambient Ne in the 1981 April 27 flare was overabundant by about a factor of 3 compared with accepted coronal and photospheric compositions. Their calculations yielded a Ne/O ratio of 0.38 compared with 0.15 for the accepted coronal and photospheric abundances. Since we find that the Ne/(C + N + O) $\gamma$-ray line ratio varies by less than a factor of 2 from flare to flare, this suggests that the "overabundance" of Ne is typical of flare plasma. The measured Ne/O ratio of 0.32 from X-ray observations of a single flare (Schmelz 1993) is the only other measurement suggesting this anomalous level of Ne. Although the Ne/O ratio in flares and active regions measured by both Saba & Strong (1993) and by McKenzie & Feldman (1992) varied significantly, its value seldom exceeded 0.20. If the accepted Ne abundances of the corona and photosphere are not in error, we need to find an alternative explanation for the high absolute value found in the $\gamma$-ray line measurements. Shemi (1991) attempted to explain this difference by postulating that Ne could be photoionized and become concentrated in the flare plasma in much the same way as the low-FIP elements are enhanced in the corona. If this were true, one would expect Ne to have a highly varying composition relative to C, N, and O, much like the low-FIP elements. This is clearly not what the $\gamma$-ray line data reveal. Also, in order to explain the relative constancy of the Ne/high-FIP line ratios found here, one would require both the presence of intense soft X-ray emission preceding all of these flares and prompt diffusion of the Ne into the flare plasma. We typically find that the onset of soft X-rays measured by the *GOES* satellites precedes the $\gamma$-rays by from 5 to 20 minutes. Whether these X-rays can produce the required photoionization on such time scales needs to be determined. One might also expect to see changes in the Ne/O ratio during the flares. This latter study is being planned using the *SMM* $\gamma$-ray data.

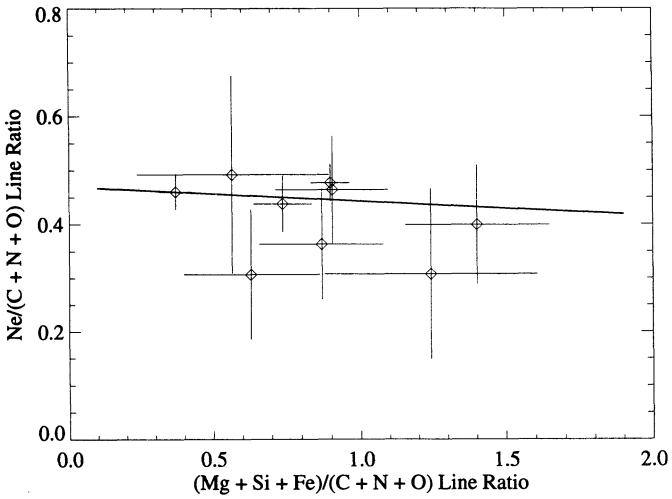


FIG. 6.—Comparison of Ne/(C + N + O) and (Mg + Si + Fe)/(C + N + O) line ratios showing that the concentrations of Ne and other high-FIP elements are relatively constant from "photospheric" to "coronal" compositions of the flare plasma, as measured by the low-FIP/high-FIP ratio.

### 4.3. *Accelerated Particle Spectra and the* Ne "*Excess*"

We seek an alternative explanation for the apparently high fluxes in the Ne $\gamma$-ray line in the 19 flares studied here. Murphy et al. (1991) assumed that the spectrum of accelerated protons and $\alpha$-particles follow a Bessel function shape arising from stochastic acceleration; they also assumed a thick-target interaction model. These assumptions produce a relatively flat spectrum near $\sim$10 MeV in the interaction region. We wish to determine whether a softer spectrum could explain the high Ne flux. We have presented evidence that both the C/O and Ne/O ratios are dependent on the spectral hardness of the accelerated particles (see Fig. 3). This is understandable in terms of differences in the excitation cross sections of C, O, and Ne at low energy (Fig. 4). We note that nuclear states producing $\gamma$-rays are excited by protons at energies down to about 3 MeV for Ne, 5 MeV for C, and 7.5 MeV for O. In contrast, we note that the cross sections for $\alpha$-particle excitation of C, O, and Ne all peak near 3 MeV nucleon$^{-1}$, with the cross section for Ne much more sharply peaked. This implies that the proton intensity may need to be significantly higher than the $\alpha$-particle intensity of below 10 MeV nucleon$^{-1}$ to explain the large Ne/O variation with spectral index. Murphy et al. (1991) obtained best fits to the 1981 April 27 data with $\alpha/p$ ratios of 0.5 to 1.0, under the assumption that the accelerated particles have the same spectral shape. If such a high ratio were characteristic of all the flares in our sample, it is not clear whether we would have observed such a striking variation in the Ne/O ratio with spectral index. Murphy et al. do obtain a smaller $\alpha/p$ ratio (0.1) with a moderately acceptable fit, but this was for a model having photospheric ambient abundances. One possible explanation is that the protons and $\alpha$-particles have different spectra.

This suggests that the presence of a steep proton spectrum of below 10 MeV in the interaction region could produce an enhancement in the yield of 1.634 MeV $\gamma$-rays from Ne relative to other lines. One needs to perform the detailed calculations similar to those in Murphy et al. (1991) to determine whether the presence of such a steep spectrum would produce the

observed Ne $\gamma$-ray line flux without violating some other features of the observed spectra. Measurements of accelerated ion spectra in interplanetary space from impulsive flares have been made by Reames, Richardson, & Wenzel (1992). Their measurements covered the particle energy range from about 0.1 to a few tens of MeV, relevant to $\gamma$-ray line production. Typical particle spectra can be fitted with power laws having spectral indices of $-3.5$ or steeper above $\sim 2$ MeV nucleon$^{-1}$. This is consistent with spectral indices obtained by comparing the 2.223 MeV/4.439 MeV line ratio (see Fig. 3); however, we note that the value of the index is dependent on the assumed accelerated and ambient particle abundances. If such a steep spectral index is representative of protons in the interaction region, a significantly increased yield of 1.634 MeV $\gamma$-rays above that estimated by Murphy et al. (1991) is expected.

We note that the Ne/O line ratio may be an excellent diagnostic for estimating the spectra of protons less than 10 MeV. This complements the 2.223 MeV/(4–7 MeV) line ratios traditionally used to estimate the low-energy proton spectra.

### 4.4. *Conclusions*

In summary, we have found that $\gamma$-ray line observations of solar flares reveal striking variability in the elemental composition of ambient material. Elements with first ionization potentials less than 10 eV vary from flare-to-flare by as much as a factor of $\sim 4$ relative to elements with higher potentials. This range is similar to the increase in low-FIP elements relative to high-FIP elements in going from the photosphere to the corona and with the varying abundances found in the solar atmosphere over different regions of the photosphere. Earlier $\gamma$-ray line analysis of the 1981 April 27 flare (Murphy et al. 1991) indicated that Ne was overabundant in the flare plasma, suggesting that this material is different in composition from either the corona or the photosphere. Our study reveals that the abundance of Ne relative to other high-FIP elements (C, N, O) in the flare plasma is constant from coronal to photospheric compositions, as measured by the high-FIP/low-FIP $\gamma$-ray line ratios. We also show that the Ne/O line ratio exhibits a significant dependence on the low-energy spectrum of accelerated particles. This effect is expected from excitation cross sections when the $\alpha/p$ ratio in the accelerated particles is small. This suggests that use of a steeper particle spectrum in the interaction region could lower the enhanced Ne abundance derived by Murphy et al. (1991). Detailed calculations are needed to confirm this suggestion.

We wish to thank Richard MacKinnon for his assistance with analysis of the data. We also acknowledge the stimulating and informative discussions we have had with Uri Feldman, Jean-Paul Meyer, Reuven Ramaty, Donald Reames, Julia Saba, and Neil Sheeley. This work is supported under NASA contract DPR W-18323.

## REFERENCES

Antiochos, S. K. 1994, Adv. Space Res., 14, No. 4, 139
Feldman, U. 1990, ApJ, 364, 322
———. 1992, Phys. Scr., 46, 202
Feldman, U., & Widing, K. G. 1990, ApJ, 363, 292
Forrest, D. J. 1983, in Positron Electron Pairs in Astrophysics, ed. M. L. Burns, A. K. Harding, & R. Ramaty (New York: AIP), 3
Forrest, D. J., et al. 1980, Sol. Phys., 65, 15
McKenzie, D. L., & Feldman, U. 1992, ApJ, 389, 764
Meyer, J. P. 1985a, ApJS, 57, 151
———. 1985b, ApJS, 57, 173
———. 1989, in AIP Conf. Proc. 183, Cosmic Abundances of Matter, ed. C. J. Waddington (New York: AIP), 245
———. 1993, in Origin and Evolution of the Elements, ed. N. Prantzos, E. Vangioni-Flam, & M. Cassé (Cambridge: Cambridge Univ. Press), 26
Murphy, R. J. 1985, Ph.D. thesis, Univ. Maryland
Murphy, R. J., Ramaty, R., Kozlovsky, B., & Reames, D. V. 1991, ApJ, 371, 793
Murphy, R. J., Share, G. H., Letaw, J. R., & Forrest, D. J. 1990, ApJ, 358, 298
Ramaty, R. 1994, private communication
Ramaty, R., & Kozlovsky, B. 1994, private communication
Ramaty, R., Kozlovsky, B., & Lingenfelter, R. E. 1979, ApJS, 40, 487
Ramaty, R., Mandzhavidze, N., Kozlovksy, B., & Skibo, J. G. 1993, Adv. Space Res., 13, No. 9, 275
Reames, D. V. 1995, Adv. Space Res., 15, No. 7, 41
Reames, D. V., Meyer, J. P., & von Rosenvinge, T. T. 1994, ApJS, 90, 649
Reames, D. V., Ramaty, R., & von Rosenvinge, T. T. 1988, ApJ, 332, L87
Reames, D. V., Richardson, I. G., & Wenzel, K.-P. 1992, ApJ, 387, 715
Rieger, E. 1994, ApJS, 90, 645
Saba, J. L. R. 1995, Adv. Space Res., 15, No. 7, 13
Saba, J. L. R., & Strong, K. T. 1993, Adv. Space Res., 13, No. 9, 391
Schmelz, J. T. 1993, ApJ, 408, 373
Shemi, A. 1991, MNRAS, 251, 221
Widing, K. G., & Feldman, U. 1993, ApJ, 416, 392
———. 1995, ApJ, 442, 446